

Three-dimensional telomere profiles in papillary thyroid cancer variants: A pilot study

Aline Rangel-Pozzo^{1#}, Tinuccia Dettori^{2#}, Daniela Virginia Frau², Federica Etzi³, John Gartner⁴, Garbor Fisher⁴, Roberta Vanni², Sabine Mai¹ and Paola Caria^{2*}

ABSTRACT

Besides the two main histologic types of papillary thyroid carcinoma (PTC), the classical PTC (CL-PTC) and the follicular variant PTC (FV-PTC), several other variants are described. The encapsulated FV-PTC variant was recently reclassified as non-invasive follicular thyroid neoplasm with papillary-like nuclear features (NIFTP) due to its similarities to benign lesions. Specific molecular signatures, however, are still unavailable. It is well known that improper DNA repair of dysfunctional telomeres may cause telomere-related genome instability. The mechanisms involved in the damaged telomere repair processing may lead to detrimental outcomes, altering the three-dimensional (3D) nuclear telomere and genome organization in cancer cells. This pilot study aimed to evaluate whether specific 3D nuclear telomere architecture might characterize NIFTP, potentially distinguishing it from other PTC histologic variants. Our findings demonstrate that 3D telomere profiles of CL-PTC and FV-PTC were different from NIFTP and that NIFTP more closely resembles follicular thyroid adenoma (FTA). NIFTP has longer telomeres than CL-PTC and FV-PTC samples, and the telomere length of NIFTP overlaps with that of the FTA histotype. In contrast, there was no association between BRAF expression and telomere length in all tested samples. These preliminary findings reinforce the view that NIFTP is closer to non-malignant thyroid nodules and confirm that PTC features short telomeres.

KEYWORDS: Papillary thyroid cancer; non-invasive follicular thyroid neoplasm with papillary-like nuclear features; follicular adenoma; 3D telomere profiles

INTRODUCTION

Thyroid cancer is one of the most common malignant endocrine neoplasms and papillary thyroid carcinoma (PTC) constitutes approximately 80% of all thyroid cancer cases [1]. The cancer genome atlas study [2] has demonstrated a strong correlation between genetic alterations and histologic phenotypes of thyroid neoplasia, resulting in the identification of two distinct molecular subgroups: The BRAFV600E-like nodules, which show the true papillary architecture, and

RAS-like nodules, with a follicular-pattern that includes follicular thyroid adenoma (FTA), follicular carcinoma, and follicular variant PTC (FV-PTC). Recently, the non-invasive follicular thyroid neoplasm with papillary-like nuclear features (NIFTP) variant [3], a very low-risk thyroid tumor previously known as an encapsulated non-invasive follicular variant PTC (EFVPTC), has been included in the RAS-like subgroup. However, no specific molecular signatures have been identified [4,5]. Although the vast majority of nodules classified as NIFTP have an overall clinical favorable behavior, lymph node metastasis has been reported in a minority of cases [4], pointing to the need for the identification of new accurate potential diagnostic parameters.

It is well known that telomeres have an essential role in preserving chromosome stability and integrity. Intact telomeres prevent end-to-end fusions, degradation of the chromosome ends, and contribute to the adequate chromosome positioning within the nucleus [6]. Studies using quantitative three-dimensional (3D) telomere imaging have shown differences in the 3D telomere architecture in the nucleus of cancer cells compared to the pattern observed in the normal cell nucleus [7-10]. Recently, we highlighted the importance of telomere-related genomic instability during the tumorigenesis of PTC. By selecting PTC-derived cell lines characteristic of PTC tumors in the BRAF^{V600E}-like subgroup, we demonstrated that isolated cancer stem-like cells (representing an early cancer-promoting subpopulation) had a trend toward lower telomere shortening compared to the corresponding parental cells (representing the

¹Department of Cell Biology, Research Institute of Oncology and Hematology, CancerCare Manitoba, University of Manitoba, Winnipeg, Canada

²Department of Biomedical Sciences, University of Cagliari, Monserrato, Italy

³Department of Biomedical Sciences-Histology, University of Sassari, Sassari, Italy

⁴Department of Pathology, Max Rady College of Medicine Rady Faculty of Health Sciences, University of Manitoba, Winnipeg, Canada

[#]These authors contributed equally to this work

*Corresponding author: Paola Caria, Department of Biomedical Sciences, University of Cagliari, Monserrato, Italy.
E-mail: paola.caria@unica.it

DOI: <https://doi.org/10.17305/bjbms.2021.6639>

Submitted: 19 October 2021/Accepted: 11 November 2021/
Published online: 30 November 2021

Conflicts of interest: S.M. is a shareholder, director and chair of the clinical and scientific advisory board of Telo Genomics Corp. (Toronto ON, Canada). The other authors declare that they have no conflicts of interest.

Funding: This work was supported by the Research Integrative Fund (FIR) of the University of Cagliari to PC, TD, and RV and the Rady Innovation Fund (SM, JG, GF, PC).



©The Author(s) (2022). This work is licensed under a Creative Commons Attribution 4.0 International License

tumor bulk cells) [11]. Literature data highlight that improper DNA repair of dysfunctional telomeres can cause telomere-related genome instability [12]. As a result, harmful outcomes can occur that alter the 3D nuclear telomere and genome organization in cancer cells [9]. On these bases, considering that the biological features of NIFTP are still unclear, possibly due to the highly variable incidence (<1-28% of all PTC) and the lack of well-established differentiation criteria [13], we designed a pilot study to investigate the potential role of 3D telomere imaging and nuclear architecture in the further characterization of this rare thyroid tumor. Although with a reduced number of cases, this pilot study indicates that NIFTP has specific 3D nuclear telomere architecture and suggests that the specific 3D pattern observed may provide an additional parameter in the differential diagnosis of indolent thyroid nodules, thereby preventing unnecessary patient treatment.

MATERIALS AND METHODS

Patient samples

A total of 15 primary thyroid tumor tissue samples were obtained from the Health Sciences Centre (Winnipeg, Manitoba, Canada). The tumor and normal adjacent tissue (NAT) of formalin-fixed paraffin-embedded (FFPE) sections (5 μm) were circled with a pen after review of the corresponding hematoxylin- and eosin-stained sections by two pathologists (JG and GF). The experiments were blinded to the tumor characteristics and outcome data. The patient cohort included in this study was composed of 3 (20%) men and 12 (80%) women ages 31-67, with a median age of 51 years. Surgical specimens were classified according to the World Health Organization classification [14]. Clinical, pathological, and molecular characteristics of the 15 patients are shown in Table 1.

3D quantitative fluorescence in situ hybridization (Q-FISH)

Nuclei from 5- μm thyroid tissue sections underwent 3D quantitative fluorescence *in situ* hybridization Q-FISH with a peptide nucleic acid-Cy3-telomere probe-(TTAGGG)_n (DAKO, Glostrup, Denmark). The hybridization procedure was performed as previously described [15]. The 3D image analysis was carried out on 100 nuclei per tumor sample using AxioImager Z2 microscope (Carl Zeiss Canada Ltd). A 63x/1.4 oil objective lens (Carl Zeiss Canada Ltd.) were used for image acquisition. Eighty z-stacks were acquired at a sampling distance of x, y: 102 nm, and z: 200 nm for each slice to create optical sections. A constant acquisition time of 300 milliseconds for Cy3 (telomeres) was used, while the exposure times for the DAPI (nuclei) varied for each sample. The constrained iterative algorithm was used for deconvolution [16]. Deconvolved

images were analyzed using the TeloView® v1.03 software program (Telo Genomics Corp., Toronto, ON, Canada) [17]. TeloView® measures six different telomere parameters in each cell, generating specific 3D telomere profiles for each thyroid sample examined [11,18].

BRAF expression and RET/PTC and PPAR γ rearrangements

BRAFV600E protein expression was detected using the anti-BRAFV600E (clone VE1) mutation-specific mouse monoclonal antibody (Abcam ab228461 Milano, Italy) in accordance with the protocol utilized in the previous studies [19]. Sequencing-validated BRAF^{V600E} mutation positive (seven samples) and negative (three samples) PTC cases [20] were used as positive and negative controls, respectively, to test clone VE1 antibody. Normal thyroid tissue from the tumor-free contralateral lobe of five PTCs was also used as control [21]. The Image J software (US National Institutes of Health, USA) was used to determine the fluorescence intensity as previously described [22]. All BRAF positive controls showed BRAF protein expression, with mean fluorescence intensity of 100 (100 \pm 10 SD) arbitrary units (a.u) ranging from 81.5 to 113, and this range of values was considered to assign the presence of BRAF^{V600E} mutation in our samples. In BRAF negative cases, the mean fluorescence intensity was 19 a.u (19 \pm 0.7 SD), ranging from 19.8 to 20.7. This range of values was used to assign the absence of BRAF^{V600E} mutation in our samples. Mean fluorescence intensity in normal thyroid tissues was in the range of BRAFV600E negative controls, corroborating this approach.

Images were obtained with an epifluorescence microscope (Olympus BX41) and charge-coupled device camera (Cohu), interfaced with the CytoVysion system (software 2.81 Applied Imaging, Pittsburg, PA, USA). In each section, tumor and normal area were evaluated, and ten randomly selected fields for each sample were acquired with a \times 100 objective.

The presence of RET/PTC and PPAR γ rearrangements was tested by FISH, using the dual-color break-apart strategy, as previously described [21].

Ethical statement

Informed written consents were collected from all the patients in accordance with the declaration of Helsinki. The protocol of this study was approved by the Health Research Ethics Board on human studies from the University of Manitoba, Canada, (HS21723; H2018:156).

Statistical analysis

To compare telomere parameters among different histology, nested factorial analysis of variance was used. We also

TABLE 1. Clinical, pathological, and molecular characteristics of patients

Case n	Sex	Age	Histotype	TNM Classification	Tumor Size (cm)	BRAF ^{V600E} expression	RET/PTC rearrangements	PPAR γ rearrangements
1	F	57	CL-PTC	pT2	3	NEG	NEG	NEG
2	F	51	CL-PTC	pT2N1Mx	3.3	NEG	NEG	NEG
3	F	57	CL-PTC	pT1	1.2	POS	NEG	NEG
4	F	47	CL-PTC	pT1aNX	1	POS	NEG	NEG
5	F	67	FV-PTC	pT3N1a	1.7	NEG	NEG	NEG
6	M	62	FV-PTC	pT1bNxMx	1	NEG	NEG	NEG
7	F	44	FV-PTC	pT2MxNX	4.2	POS	NEG	NEG
8	M	40	NIFTP	NA	2.2	NEG	NEG	NEG
9	F	66	NIFTP	NA	1.5	NEG	NEG	NEG
10	F	31	NIFTP	NA	1.3	NEG	NEG	NEG
11	M	39	NIFTP	NA	3.5	NEG	NEG	NEG
12	F	40	FTA	NA	3.6	NEG	NEG	NEG
13	F	54	FTA	NA	5	NEG	NEG	NEG
14	F	62	FTA	NA	1.6	NEG	NEG	NEG
15	F	31	FTA	NA	4.2	NEG	NEG	NEG

F: Female; FTA: Follicular thyroid adenoma; FV-PTC: Follicular variant of papillary thyroid carcinoma; NA: Not applicable; NIFTP: Non-invasive follicular thyroid neoplasm with papillary-like nuclear features; NEG: Negative; POS: Positive; CL-PTC: Classical papillary thyroid carcinoma

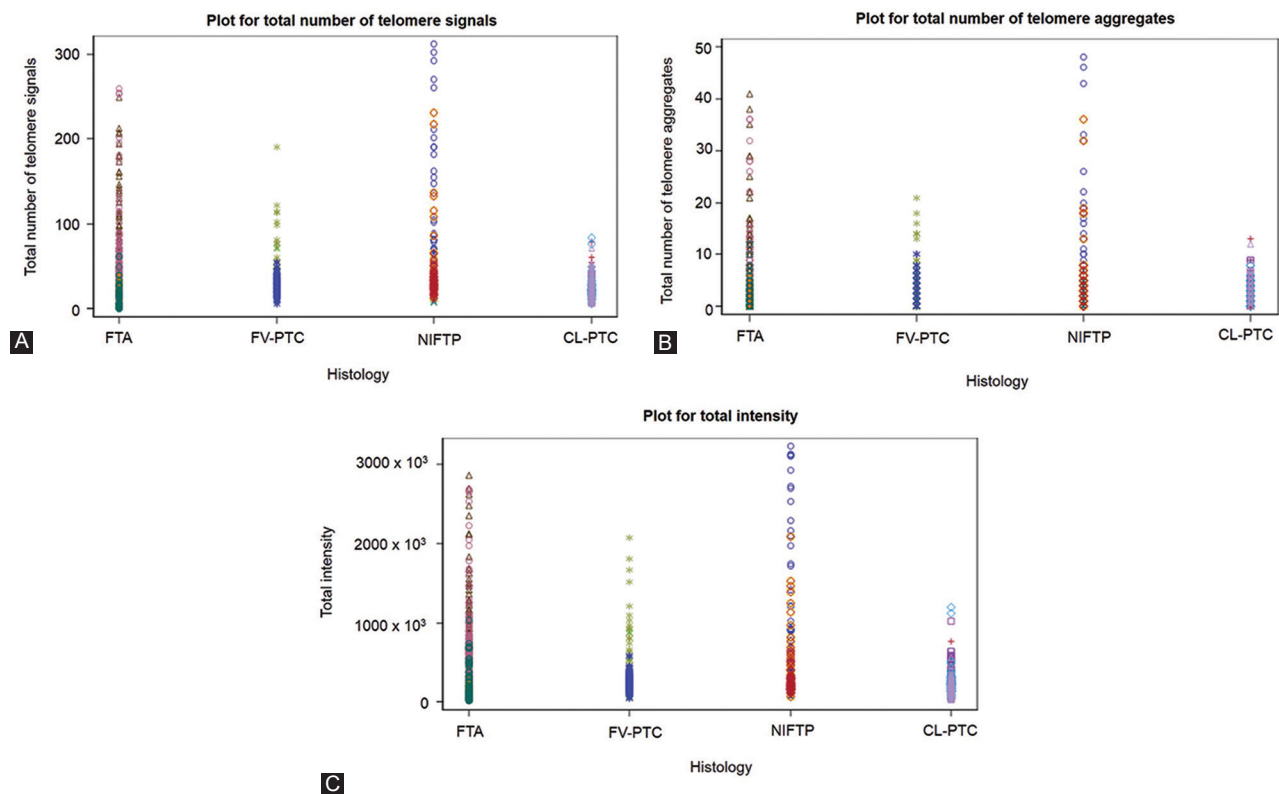


FIGURE 1. Dot plot of telomere parameters for FTA, FV-PTC, NIFTP, and CL-PTC cases. Each cell analyzed per histotype is represented in the graph. (A) Total number of telomere signals – a sum value representing the number of telomeres found in each cell population. (B) Total number of telomere aggregates – telomeres in proximity forming clusters that cannot be further resolved at an optical resolution limit of 200 nm – which, functionally, are fused telomere signals or telomeres in close illegitimate proximity able to engage in recombination events. (C) Total telomere signal intensity (proportional to telomere length). The x-axis shows values for each parameter and the y-axis refers to the cells analyzed in each histotype. FTA: Follicular adenoma; FV-PTC: Follicular variant papillary thyroid carcinoma; NIFTP: Noninvasive follicular thyroid neoplasm with papillary-like nuclear features; CL-PTC: Classical-papillary thyroid carcinoma.

compared telomere features of cells from NAT and from tumor area for each patient with a different histology using the Wilcoxon rank sum tests. Significance levels were set at $p = 0.05$.

RESULTS

3D telomere profiles in different PTC histotypes

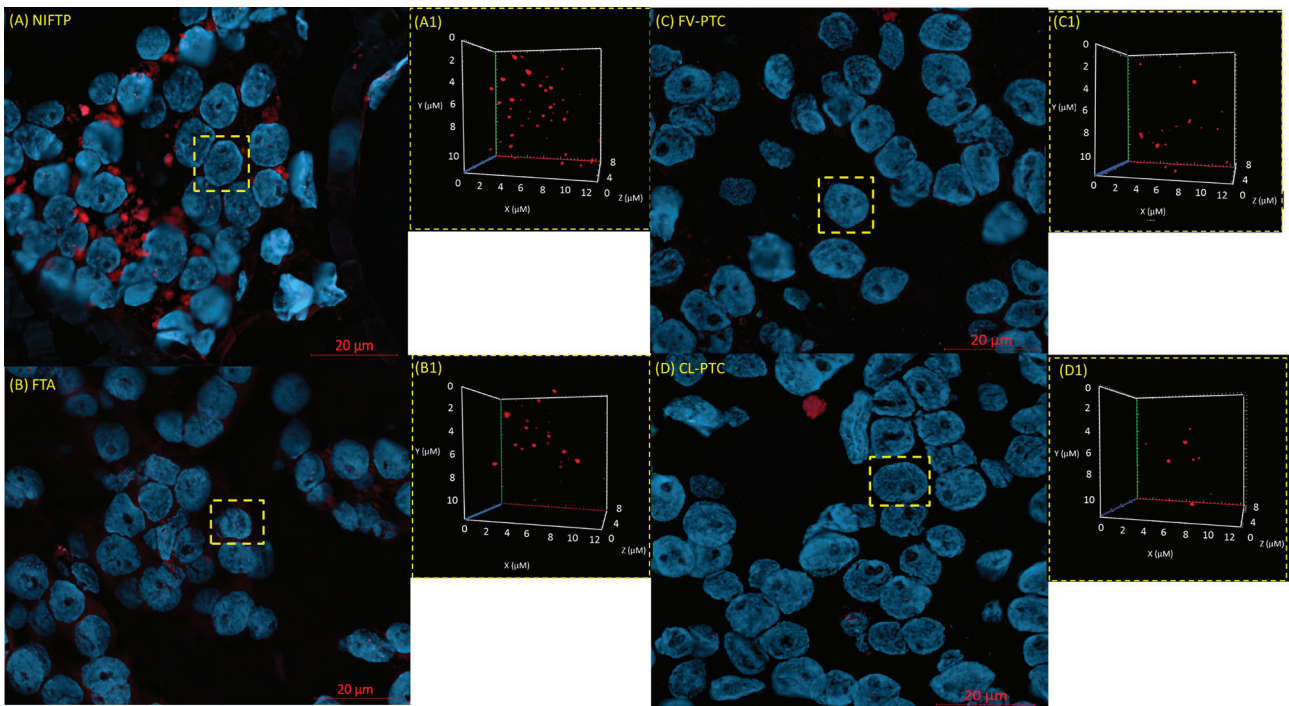


FIGURE 2. Differences in the 3D nuclear telomere architecture between NIFTP (A), FTA (B), FV-PTC (C), and CL-PTC (D). Representative nuclei, counterstained with DAPI (blue), are shown for each histotype. Cy-3 labeled telomeres appear as red signals in the 3D figures in A1, B1, C1, and D1. NIFTP: Non-invasive follicular thyroid neoplasm with papillary-like nuclear features; FTA: Follicular adenoma; FV-PTC: Follicular variant papillary thyroid carcinoma; CL-PTC: Classical-papillary thyroid carcinoma, 3D: Three-dimensional.

In the present pilot study, we examined 15 FFPE thyroid neoplasms comprising classical PTC (CL-PTC) (n = 4), FV-PTC (n = 3), NIFTP (n = 4), and FTA (n = 4). We compared their respective telomere parameters across and found a pattern differentiating FTA and NIFTP from FV-PTC and CL-PTC. FV-PTC and CL-PTC presented lower numbers of telomere signals, lower numbers of telomere aggregates, and lower total intensity when compared with FTA and NIFTP (Figures 1A-C and 2).

TeloView® analysis, creating distributions based on the frequency of telomere signals with specific intensity, enabled us to distinguish four quartiles, in arbitrary units (a.u.), indicating four cell subpopulations: Cells with very short telomeres (≤ 4000 a.u.), cells with short telomeres (4001-7000 a.u.), cells with medium telomeres (7001-13000 a.u.), and cells with large telomeres ($>13,000$ a.u.). The frequency distribution of very short telomeres (≤ 4000 a.u.) showed a significant difference between the histotypes FTA and NIFTP versus CL-PTC and FV-PTC histotypes (Figure 3). Indeed, no significant differences were observed between FTA and NIFTP or between CL-PTC and FV-PTC, NIFTP paralleling FTA telomere length while having longer telomeres compared to CL-PTC and FV-PTC. The analysis of the 3D telomere profiles in NAT showed that the most of the telomere parameters were different between NAT and FTA tumor area and NAT and NIFTP tumor area, whereas number of telomeres signals and total intensity were significantly

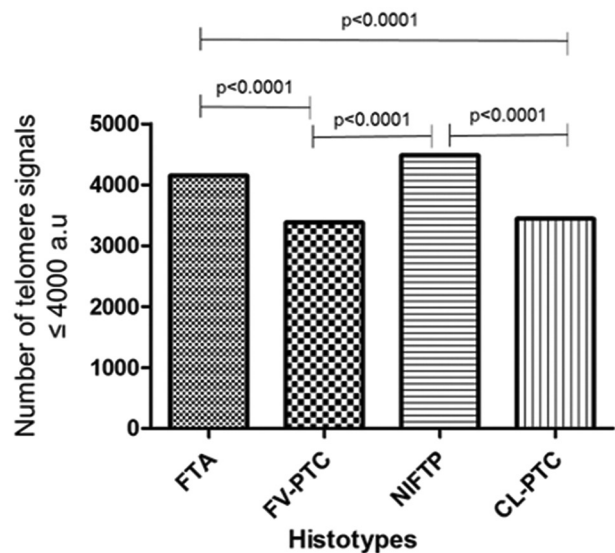


FIGURE 3. Bar plot of the differences in number of telomeres ≤ 4000 a.u. (arbitrary units) between CL-PTC, FV-PTC, FTA, and NIFTP. Cells with intensity of ≤ 4000 a.u. represent very short telomeres. The x-axis assigns one box for each cell population analyzed (results of all analyzed cells). The y-axis refers to the number of telomeres ≤ 4000 a.u. (showing only the significant *p* values). CL-PTC: Classical-papillary thyroid carcinoma; FV-PTC: Follicular variant papillary thyroid carcinoma; FTA: Follicular adenoma; NIFTP: Non-invasive follicular thyroid neoplasm with papillary-like nuclear features.

different between NAT and CL-PTC tumor area, and the average intensity was different between NAT and FV-PTC (Table 2).

TABLE 2. Three-dimensional telomere parameters of thyroid tumor versus normal to adjacent tumor tissue

Histotype	Number of telomere signals	Number of telomere aggregates	Average intensity	Total intensity
CL-PTC	$p < 0.001$ (\downarrow NNTA \times T \uparrow)	NS	NS	$p = 0.0365$ (\downarrow NNTA \times T \uparrow)
FV-PTC	NS	NS	$p < 0.001$ (\uparrow NNTA \times T \downarrow)	Ns
NIFTP	$p < 0.001$ (\uparrow NNTA \times T \downarrow)	$p < 0.001$ (\downarrow NNTA \times T \uparrow)	Ns	$p < 0.001$ (\uparrow NNTA \times T \downarrow)
FTA	$p < 0.001$ (\downarrow NNTA \times T \uparrow)	$p < 0.001$ (\downarrow NNTA \times T \uparrow)	$p = 0.0106$ (\downarrow NNTA \times T \uparrow)	$p < 0.001$ (\downarrow NNTA \times T \uparrow)

CL-PTC: Classical-papillary thyroid carcinoma; FV-PTC: Follicular variant papillary thyroid carcinoma; NIFTP: Non-invasive follicular thyroid neoplasm with papillary-like nuclear features; FTA: Follicular adenoma; NAT: Normal tissue adjacent to the tumor; T: Tumor; \uparrow increase; \downarrow decrease; NS: Not significant

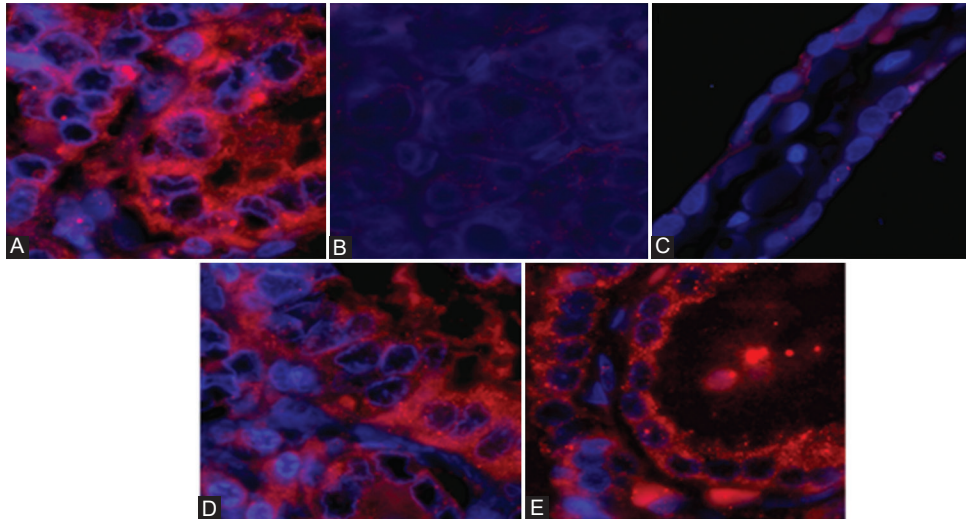


FIGURE 4. Representative images of BRAFV600E (VE1) immunofluorescence staining. BRAFV600E – mutant PTC case (A), BRAFV600E – wild type PTC (B), and normal thyroid tissue (C), CL-PTC and FV-PTC with an unequivocal diffuse cytoplasmic staining with the VE1 antibody in the majority of tumor cells (D and E). PTC: Papillary thyroid carcinoma.

BRAF^{V600E} expression and RET/PTC and PPAR γ rearrangements

BRAF protein expression was indicative of BRAFV600E mutation in three out of 15 cases. The three cases (two CL-PTC and one FV-PTC) showed unequivocal diffuse cytoplasmic antibody fluorescence intensity between 81 and 86.5 a.u. in the majority of tumor cells (Figure 4). Analysis for possible RET and PPAR γ rearrangements accomplished by dual-color break-apart probe FISH was negative in all cases.

DISCUSSION

Noninvasive follicular thyroid neoplasm with papillary-like nuclear features (NIFTP), previously known as EFVPTC, displays cells with features that look like PTC but are considered to have an extremely low risk of adverse outcomes. NIFTP tumor diagnosis must meet very stringent morphological criteria since no specific markers are available nor molecular signatures have been defined, although NIFTP falls among the RAS-like papillary tumors [4]. In this context, we designed a pilot study to investigate the 3D telomere profiles of malignant PTC variants and benign FTA to assess whether NIFTP 3D telomere profiles could be evaluated as a possible ancillary parameter in the characterization of this low-risk tumor variant.

We counted lower numbers of telomeres and shorter telomeres in CL-PTC and FV-PTC variants than NIFTP and FTA. This result suggests the decrease in the number of telomeres as a consequence of telomere shortening since fewer telomeres (TTAGGG) repeats would be available for probe binding. This observation is in line with the previous studies indicating the association of short telomeres with classic and follicular variants of PTC and long telomeres with benign thyroid nodules [23,24]. Dot plot profile showing higher numbers of telomere aggregates for FTA and NIFTP compared to FV-PTC and CL-PTC cases corroborates this view. Indeed, the aggregates observed in FTA and NIFTP may represent the telomere associations seen in classical cytogenetic studies [25,26]. Our data, indicating that the investigated NIFTP has telomere signatures similar to FTA and dissimilar from CL-PTC and FV-PTC, reinforce the idea that NIFTP is more closely related to benign thyroid neoplasm rather than to malignant lesions [27,28]. In addition, our NIFTP cases were negative for BRAFV600E, according to the lack of this mutation in NIFTP [29].

Considering that telomeres length in healthy tissue can vary significantly from one patient to another, we also analyzed the 3D telomere profiles in NAT. In general, the most of the 3D telomere profile parameters differed between NAT and tumor areas of FTA and NIFTP, indicating a clear-cut

separation between the profiles of normal tissue cells and cells of these two nodule variants contained within the tumor capsule. On the contrary, in the malignant tumors, among the 3D telomeres parameters analyzed, we found that only the number of telomeres and total intensity were significantly different between NAT and CL-PTC tumor areas. In contrast, between FV-PTC and the respective NAT, only the average intensity was different. The finding of this altered feature in the surrounding-tumor cells with apparently normal morphology suggests that the alteration is an early molecular event preceding changes visible at the histological level.

CONCLUSION

In summary, our preliminary data show that 3D telomere organization of NIFTP is similar to that of benign FTA, and it is dissimilar from that of classical and follicular variant PTC. These findings are in line with the view that NIFTP is a lesion closer to non-malignant thyroid nodules and confirmed that short telomeres are a feature of PTC. It is of note that, in keeping with the stringent criteria for NIFTP diagnosis, our NIFTP samples are negative for both BRAF and RET alterations.

Our first study of 3D nuclear telomere organization in PTC primary tumor variants provides a strong rationale for additional studies in a larger cohort. If confirmed, our findings are a promising tool to be considered among the strict parameters required to reach the exact diagnosis of NIFTP, enabling predicting the outcome of this tumor and patient-specific clinical management.

ACKNOWLEDGMENTS

Acknowledgments: The authors would like to thank Telo Genomics Corp. for the use of TeloView® software platform, Mary Cheang for the statistical analysis, and Elizabete Cruz for helping in the manuscript preparation. The authors also thank the Genomic Centre for Cancer Research and Diagnosis (GCCRD) for imaging. The GCCRD is funded by the Canada Foundation for Innovation and supported by CancerCare Manitoba Foundation, the University of Manitoba, and a Canada Research Chair Tier 1 (SM). The GCCRD is a member of the Canadian National Scientific Platforms (CNSP) and of Canada BioImaging. The authors thank the Department of Pathology - Health Sciences Centre (Winnipeg, Manitoba, Canada) for supporting this project with thyroid tissue samples.

REFERENCES

[1] Davies L, Welch HG. Increasing incidence of thyroid cancer in the United States. *JAMA* 2006;295(18):2164-7. <https://doi.org/10.1001/jama.295.18.2164>

[2] Cancer Genome Atlas Research Network. Integrated genomic characterization of papillary thyroid carcinoma. *Cell* 2014;159(3):676-90. <https://doi.org/10.1016/j.cell.2014.09.050>

[3] Nikiforov YE, Seethala RR, Tallini G, Baloch ZW, Basolo F, Thompson LD, et al. Nomenclature revision for encapsulated follicular variant of papillary thyroid carcinoma: A paradigm shift to reduce overtreatment of indolent tumors. *JAMA Oncol* 2016;2(8):1023-9. <https://doi.org/10.1001/jamaoncol.2016.0386>

[4] Alves VA, Kakudo K, LiVolsi V, Lloyd RV, Nikiforov YE, Nosé V, et al. Noninvasive follicular thyroid neoplasm with papillary-like nuclear features (NIFTP): Achieving better agreement by refining diagnostic criteria. *Clinics (Sao Paulo)* 2018;73:e576. <https://doi.org/10.6061/clinics/2018/e576>

[5] Liu J, Singh B, Tallini G, Carlson DL, Katabi N, Saha A, et al. Follicular variant of papillary thyroid carcinoma: A clinicopathologic study of a problematic entity. *Cancer* 2006;107(6):1255-644. <https://doi.org/10.1002/cncr.22138>

[6] de Lange T. How telomere solve the end-protection problem. *Science* 2009;326(5955):948-52. <https://doi.org/10.1126/science.1170633>

[7] Klewes L, Vallente R, Dupas E, Carolin B, Grün D, Guffei A, et al. Three-dimensional nuclear telomere organization in multiple myeloma. *Transl Oncol* 2013;6(6):749-56. <https://doi.org/10.1937/tlo.13613>

[8] Knecht H, Sawan B, Lichtensztein D, Lemieux B, Wellinger RJ, Mai S. The 3D nuclear organization of telomeres marks the transition from hodgkin to reed-sternberg cells. *Leukemia* 2009;23(3):565-73. <https://doi.org/10.1038/leu.2008.314>

[9] Kuzyk A, Gartner J, Mai S. Identification of neuroblastoma subgroups based on three-dimensional telomere organization. *Transl Oncol* 2016;9(4):348-56. <https://doi.org/10.1016/j.tranon.2016.07.001>

[10] Louis SF, Vermolen BJ, Garini Y, Young IT, Guffei A, Lichtensztein Z, et al. c-Myc induces chromosomal rearrangements through telomere and chromosome remodeling in the interphase nucleus. *Proc Natl Acad Sci USA* 2005;102(27):9613-8. <https://doi.org/10.1073/pnas.0407512102>

[11] Caria P, Dettori T, Frau DV, Lichtensztein D, Pani F, Vanni R, et al. Characterizing the three-dimensional organization of telomeres in papillary thyroid carcinoma cells. *J Cell Physiol* 2019;234(4):5175-85. <https://doi.org/10.1002/jcp.27321>

[12] Longhese MP. DNA damage response at functional and dysfunctional telomeres. *Genes Dev* 2008;22(2):125-40. <https://doi.org/10.1101/gad.1626908>

[13] Cubero Rego D, Lee H, Boguniewicz A, Jennings TA. Noninvasive follicular thyroid neoplasm with papillary-like nuclear features (NIFTP) is rare, benign lesion using modified stringent diagnostic criteria: Reclassification and outcome study. *Ann Diagn Pathol* 2020;44:151439. <https://doi.org/10.1016/j.anndiagpath.2019.151439>

[14] Lloyd RV, Osamura TY, Kloppel G, Rosi JE. Classification of Tumours of Endocrine Organs. 4th ed., Vol. 10. Lyon, France: IARC Press; 2017.

[15] Sisdelli L, Cordioli MIV, Vaisman F, Monte O, Longui CA, Cury AN, et al. A multifocal pediatric papillary thyroid carcinoma (PTC) harboring the AGK-BRAF and RET/PTC3 fusion in a mutually exclusive pattern reveals distinct levels of genomic instability and nuclear organization. *Biology (Basel)* 2021;10(2):125. <https://doi.org/10.3390/biology10020125>

[16] Schaefer LH, Schuster D, Herz H. Generalized approach for accelerated maximum likelihood-based image restoration applied to three-dimensional fluorescence microscopy. *J Microsc* 2001;204(2):99-107. <https://doi.org/10.1046/j.1365-2818.2001.00949.x>

[17] Vermolen BJ, Garini Y, Mai S, Mougey V, Fest T, Chuang TC, et al. Characterizing the three-dimensional organization of telomeres. *Cytometry A* 2005;67(2):144-50. <https://doi.org/10.1002/cyto.a.20159>

[18] Rangel-Pozzo A, de Souza DC, Schmid-Braz AT, de Azambuja AP,

- Ferraz-Aguar T, Borgonovo T, et al. 3D telomere structure analysis to detect genomic instability and cytogenetic evolution myelodysplastic syndromes. *Cells* 2019;8(4):304. <https://doi.org/10.3390/cells8040304>
- [19] Contu F, Rangel-Pozzo A, Trokajlo P, Wark L, Klewes L, Johnson NA, et al. Distinct 3D structural patterns of lamin A/C expression in hodgkin and reed-sternberg cells. *Cancers (Basel)* 2018;10(9):286. <https://doi.org/10.3390/cancers10090286>
- [20] Caria P, Cantara S, Frau DV, Pacini F, Vanni R, Dettori T. Genetic heterogeneity of HER2 amplification and telomere shortening in papillary thyroid carcinoma. *Int J Mol Sci* 2016;17(10):1759. <https://doi.org/10.3390/ijms17101759>
- [21] Caria P, Dettori T, Frau DV, Borghero A, Cappai A, Riola A, et al. Assessing RET/PTC in thyroid nodule fine-needle aspirates: The FISH point of view. *Endocr Relat Cancer* 2013;20(4):527-36. <https://doi.org/10.1530/ERC-13-0157>
- [22] Costa G, Morelli M, Simola M. Progression and persistence of neurotoxicity induced by MDMA in dopaminergic regions of the mouse brain and association with noradrenergic, GABAergic, and serotonergic damage. *Neurotox Res* 2017;32(4):563-74. <https://doi.org/10.1007/s12640-017-9761-6>
- [23] Wang Y, Meeker AK, Kowalski J, Tsai HL, Somervell H, Heaphy C, et al. Telomere length is related to alternative splice patterns of telomerase in thyroid tumors. *Am J Pathol* 2011;179(3):1415-24. <https://doi.org/10.1016/j.ajpath.2011.05.056>
- [24] Capezzone M, Cantara S, Marchisotta S, Busonero G, Formici C, Benigni M, et al. Telomere length in neoplastic and nonneoplastic tissues of patients with familial and sporadic papillary thyroid cancer. *J Clin Endocrinol Metab* 2011;96(11):1852-6. <https://doi.org/10.1210/jc.2011-1003>
- [25] Caporali A, Wark L, Vermolen BJ, Garini Y, Mai S. Telomere aggregates and end-to-end chromosomal fusions require myc box II. *Oncogene* 2007;26(10):1398-406.
- [26] Caria P, Vanni R. Cytogenetic and molecular events in adenoma and well-differentiated thyroid follicular-cell neoplasia. *Cancer Genet Cytogenet* 2010;203(1):21-9. <https://doi.org/10.1016/j.cancergencyto.2010.08.025>
- [27] Amendoeira I, Maia T, Sobrinho-Simões M. Noninvasive follicular thyroid neoplasm with papillary-like nuclear features (NIFTP): Impact on the reclassification of thyroid nodules. *Endocr Relat Cancer* 2018;25(4):R247-58. <https://doi.org/10.1530/ERC-17-0513>
- [28] Zajkowska K, Kopczyński J, Gózdź S, Kowalska A. Noninvasive follicular thyroid neoplasm with papillary-like nuclear features: A problematic entity. *Endocr Connect* 2020;9(3):R47-58. <https://doi.org/10.1530/EC-19-0566>
- [29] Johnson DN, Sadow PM. Exploration of BRAFV600E as a diagnostic adjuvant in the noninvasive follicular thyroid neoplasm with papillary-like nuclear features (NIFTP). *Hum Pathol* 2018;82:32-8. <https://doi.org/10.1016/j.humpath.2018.06.033>

Related articles published in BJBMS

1. [Follicular morphological characteristics may be associated with invasion in follicular thyroid neoplasms with papillary-like nuclear features](#)
Nuray Can et al., BJBMS, 2017
2. [Downregulation of TSPAN13 by miR-369-3p inhibits cell proliferation in papillary thyroid cancer \(PTC\)](#)
Peng Li et al., BJBMS, 2019